CKM-TRIANGLE ANALYSIS:
Updates and Novelties for Summer 2004

UT*fit* Collaboration :

M. Bona[(a)], M. Ciuchini[(b)], E. Franco[(c)], V. Lubicz[(b)], G. Martinelli[(c)], F. Parodi[(d)], M. Pierini[(c)], P. Roudeau[(e)], C. Schiavi[(d)], L. Silvestrini[(c)] and A. Stocchi[(e)]

[(a)] **INFN, Sezione di Torino,**
Via P. Giuria 1, I-10125 Torino, Italy
[(b)] **Università di Roma Tre and INFN, Sezione di Roma III,**
Via della Vasca Navale 84, I-00146 Roma, Italy
[(c)] **Università di Roma "La Sapienza" and INFN, Sezione di Roma,**
Piazzale A. Moro 2, 00185 Roma, Italy
[(d)] **Dipartimento di Fisica, Università di Genova and INFN**
Via Dodecaneso 33, 16146 Genova, Italy
[(e)] **Laboratoire de l'Accélérateur Linéaire**
IN2P3-CNRS et Université de Paris-Sud, BP 34, F-91898 Orsay Cedex

Abstract

Using the most recent determinations of several theoretical and experimental parameters, we update the Unitarity Triangle analysis in the Standard Model. The basic experimental constraints come from the measurements of ε_K, $|V_{ub}/V_{cb}|$, and Δm_d, the limit on Δm_s, and the measurement of the CP asymmetry in the B sector through the $J/\psi K^0$ channel. In addition we also include in our analysis the direct determination of $\sin 2\alpha$, γ, and $\sin(2\beta+\gamma)$ from the measurements of new CP-violating quantities, recently coming from the B-Factories. We also discuss the opportunities offered by improving the precision of the measurements of the various physical quantities entering in the determination of the Unitarity Triangle parameters.

The results and the plots presented in this paper can be also found at the URL `http://www.utfit.org`, where they are continuously updated with the newest experimental and theoretical results [1].

Submitted to the 32nd International Conference on High-Energy Physics, ICHEP 04, 16 August—22 August 2004, Beijing, China

1 Introduction

The analysis of the Unitarity Triangle (UT) and CP violation represents one of the most stringent tests of the Standard Model (SM) and, for this reason, it is also an interesting window on New Physics (NP). The most precise determination of the parameters governing this phenomenon is obtained using B decays, $B^0 - \overline{B^0}$ oscillations and CP asymmetries in the kaon and in the B sectors.

Up to now, the standard analysis [2, 3] relies on the following measurements: $|V_{ub}| / |V_{cb}|$, Δm_d, the limit on Δm_s, and the measurements of CP-violating quantities in the kaon (ε_K) and in the B ($\sin 2\beta$) sectors. Inputs to this analysis constitute a large body of both experimental measurements and theoretically determined parameters, where Lattice QCD calculations play a central role. A careful choice (and a continuous update) of the values of these parameters is a prerequisite in this study. The values and errors attributed to these parameters are summarized in Table 1 (Section 2).

The results of the analysis and the determination of the UT parameters are presented and discussed in Section 3 which is an update of similar analyses performed in [2] to which the readers can refer for more details.

New CP-violating quantities have been recently measured by the B-Factories, allowing for the determination of several combinations of UT angles. The measurements of $\sin 2\alpha$, γ, and $\sin(2\beta+\gamma)$ are now available using B decays into $\pi\pi$ and $\rho\rho$, $D^{(*)}K$ and $D^{(*)}\pi$ final states, respectively. These measurements are presented in Section 4 and their effect on the UT fit is discussed in Section 4.4.

Finally we also discuss the perspectives opened by improving the precision in the measurements of various physical quantities entering the UT analysis. In particular, we investigate to which extent future and improved determinations of the experimental constraints, such as $\sin 2\beta$, Δm_s and γ, could allow us to invalidate the SM, thus signaling the presence of NP effects.

2 Inputs used for the "Standard" analysis

The values and errors of the relevant quantities entering the standard analysis of the CKM parameters (corresponding to the constraints from $|V_{ub}| / |V_{cb}|$, Δm_d, $\Delta m_s/\Delta m_d$, ε_K and $\sin 2\beta$) are summarized in Table 1.

The novelties here are the final LEP/SLD likelihood from Δm_s, the value of $|V_{ub}|$ from inclusive semileptonic decays [4], the new value of $\sin 2\beta$ and a new treatment of the non-perturbative QCD parameters as explained in the following section 2.1.

2.1 Use of ξ, $f_{B_s}\sqrt{\hat{B}_{B_s}}$ and $f_{B_d}\sqrt{\hat{B}_{B_d}}$ in Δm_s and Δm_d constraints

One of the important differences with respect to previous studies is in the use of the information from non-perturbative QCD parameters entering the expressions of Δm_s and Δm_d. The $B_s^0 - \overline{B_s^0}$ time oscillation frequency, which can be related to the mass difference between the light and heavy mass eigenstates of the $B_s^0 - \overline{B_s^0}$ system, is proportional to the square of the $|V_{ts}|$ element. Up to Cabibbo suppressed corrections, $|V_{ts}|$ is independent of $\overline{\rho}$ and $\overline{\eta}$. As a consequence, the measurement of Δm_s would provide a strong constraint on the non-perturbative QCD parameter $f_{B_s}^2 \hat{B}_{B_s}$.

Parameter	Value	Gaussian (σ)	Uniform (half-width)
λ	0.2265	0.0020	-
$\|V_{cb}\|$(excl.)	42.1×10^{-3}	2.1×10^{-3}	-
$\|V_{cb}\|$(incl.)	41.4×10^{-3}	0.7×10^{-3}	0.6×10^{-3}
$\|V_{ub}\|$(excl.)	33.0×10^{-4}	2.4×10^{-4}	4.6×10^{-4}
$\|V_{ub}\|$(incl.-LEP)	40.9×10^{-4}	6.2×10^{-4}	4.7×10^{-4}
$\|V_{ub}\|$(incl.-HFAG)	45.7×10^{-4}	6.1×10^{-4}	-
Δm_d	0.503 ps^{-1}	0.006 ps^{-1}	-
Δm_s	> 14.5 ps^{-1} at 95% C.L.	sensitivity 18.3 ps^{-1}	
m_t	167 GeV	5 GeV	-
$f_{B_s}\sqrt{\hat{B}_{B_s}}$	276 MeV	38 MeV	-
$\xi = \frac{f_{B_s}\sqrt{\hat{B}_{B_s}}}{f_{B_d}\sqrt{\hat{B}_{B_d}}}$	1.24	0.04	$\pm$ 0.06
η_b	0.55	0.01	-
$\hat{B}_K$	0.86	0.06	0.14
ε_K	2.280×10^{-3}	0.013×10^{-3}	-
η_1	1.38	0.53	-
η_2	0.574	0.004	-
η_3	0.47	0.04	-
f_K	0.159 GeV	fixed	
Δm_K	0.5301 $\times 10^{-2}$ ps^{-1}	fixed	
$\sin 2\beta$	0.739	0.048	-
m_b	4.21 GeV	0.08 GeV	-
m_c	1.3 GeV	0.1 GeV	-
α_s	0.119	0.03	-
G_F	1.16639 $\times 10^{-5}$GeV^{-2}	fixed	
m_W	80.22 GeV	fixed	
$m_{B_d^0}$	5.279 GeV	fixed	
$m_{B_s^0}$	5.375 GeV	fixed	
m_K	0.493677 GeV	fixed	

Table 1: *Values of the relevant quantities used in the fit of the CKM parameters. In the third and fourth columns the Gaussian and the flat contributions to the uncertainty are given respectively (for details on the statistical treatment see [2]). The central values and errors are those adopted at the end of the "CKM Unitarity Triangle" Workshops ([5], [6]) and by the HFAG [4].*

For this reason we propose a new and more appropriate way of treating the constraints coming from the measurements of Δm_s and Δm_d. In previous analyses, these constraints were implemented using the following equations:

$$\begin{aligned} \Delta m_d &\propto [(1-\overline{\rho})^2+\overline{\eta}^2] f_{B_d}^2 \hat{B}_{B_d} \\ \Delta m_s &\propto f_{B_s}^2 \hat{B}_{B_s} = f_{B_d}^2 \hat{B}_{B_d} \times \xi^2 \end{aligned} \tag{1}$$

where $\xi = f_{B_s}\sqrt{\hat{B}_{B_s}}/f_{B_d}\sqrt{\hat{B}_{B_d}}$. In this case the input quantities are $f_{B_d}\sqrt{\hat{B}_{B_d}}$ and ξ. The constraints from Δm_s and the knowledge of ξ are used to improve the knowledge on $f_{B_d}\sqrt{\hat{B}_{B_d}}$ which thus makes the constraint on Δm_d more effective. The main problem of this method is that the quantity that we know best from Lattice calculations is $f_{B_s}^2\hat{B}_{B_s}$, whereas ξ^2 and $f_{B_d}^2\hat{B}_{B_d}$ are affected by large uncertainties coming from chiral extrapolations. We thus suggest to use a different method which consists in writing the constraints in the following way:

$$\begin{aligned} \Delta m_d &\propto [(1-\overline{\rho})^2+\overline{\eta}^2] \frac{f_{B_s}^2 \hat{B}_{B_s}}{\xi^2} \\ \Delta m_s &\propto f_{B_s}^2 \hat{B}_{B_s} \end{aligned} \tag{2}$$

At present, this new parameterization does not have a large effect on final results but, in the future, the measurement of Δm_s will allow the elimination of a further theoretical parameter, $f_{B_s}^2\hat{B}_{B_s}$, from the UT fits. To obtain a more effective constraint on Δm_d, also the error on ξ should be improved.

3 Determination of the Unitarity Triangle parameters

In this section, assuming the validity of the Standard Model, we give the results for the quantities defining the Unitarity Triangle: $\overline{\rho}$, $\overline{\eta}$, $\sin 2\beta$, $\sin 2\alpha$, γ, $\sin(2\beta+\gamma)$ as well as other quantities such as Δm_s, $f_{B_s}\sqrt{\hat{B}_{B_s}}$, $\hat{B}_K$ and ξ. The inputs are summarized in Table 1.

3.1 Fundamental test of the Standard Model in the fermion sector

The most crucial test consists in the comparison between the $(\overline{\rho}-\overline{\eta})$ region selected by the measurements which are sensitive only to the sides of the Unitarity Triangle (semileptonic B decays and $\mathrm{B}^0-\overline{\mathrm{B}^0}$ oscillations) and the regions selected by the direct measurements of CP violation in the kaon (ε_K) or in the B ($\sin 2\beta$) sectors. This test is shown in Figure 1. It can be translated quantitatively through the comparison between the value of $\sin 2\beta$ obtained from the measurement of the CP asymmetry in $J/\psi K^0$ decays and the one determined from "sides" measurements:

$$\begin{aligned} \sin 2\beta = &\ 0.724 \pm 0.049\ [0.613; 0.803] \text{ at } 95\%\ C.L. \quad \text{sides only} \\ \sin 2\beta = &\ 0.739 \pm 0.048\ [0.681; 0.787] \text{ at } 95\%\ C.L. \quad \mathrm{J}/\psi\mathrm{K}^0. \end{aligned} \tag{3}$$

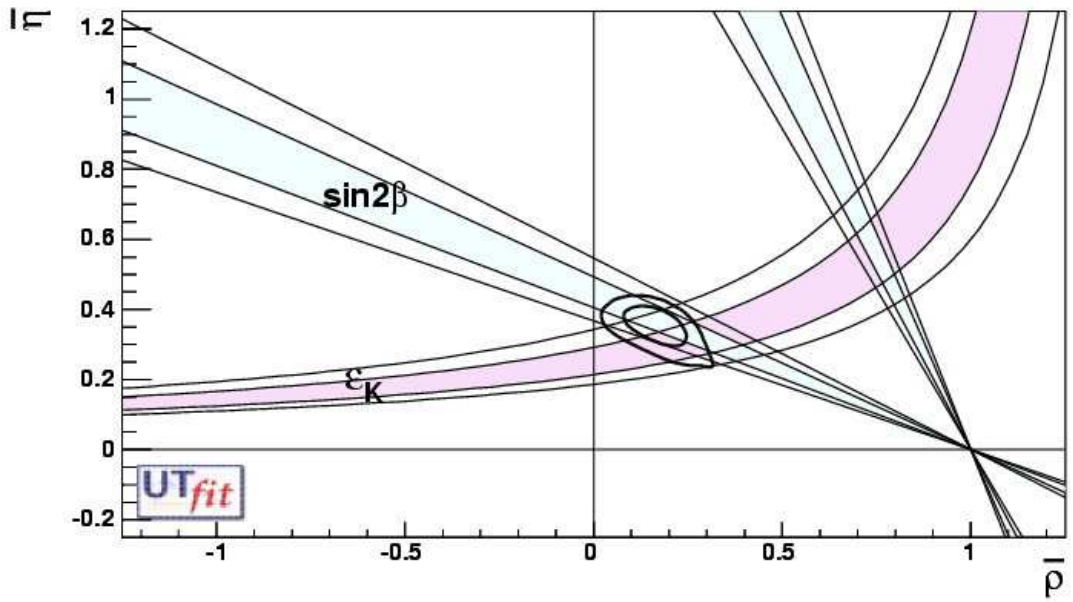

Figure 1: *The allowed regions for $\overline{\rho}$ and $\overline{\eta}$ (contours at 68%, 95% probability ranges), as selected by the measurements of $|V_{ub}|/|V_{cb}|$, Δm_d, and by the limit on $\Delta m_s/\Delta m_d$, are compared with the bands (at 68% and 95% probability ranges) from the measurements of CP-violating quantities in the kaon (ε_K) and in the B ($\sin 2\beta$) sectors.*

The spectacular agreement between these values illustrates the consistency of the Standard Model in describing CP violation phenomena in terms of one single parameter $\overline{\eta}$. It is also an important test of the Operator Product Expansion (OPE), the Heavy Quark Effective Theory (HQET) and Lattice QCD (LQCD) which have been used to extract the CKM parameters. It has to be noted that this test is even more significant because the errors on $\sin 2\beta$ from the two determinations are comparable[1].

As a matter of fact, the value of $\sin 2\beta$ was predicted, before its first direct measurement was obtained, by using all other available constraints, ($|V_{ub}|/|V_{cb}|$, ε_K, Δm_d and Δm_s). The "indirect" determination has improved regularly over the years. Figure 2 shows this evolution for the "indirect" determination of $\sin 2\beta$ which is compared with the recent determinations of $\sin 2\beta$ from direct measurements.

3.2 Determination of the Unitarity Triangle parameters

Using the constraints from $|V_{ub}|/|V_{cb}|$, Δm_d, $\Delta m_s/\Delta m_d$, ε_K and $\sin 2\beta$, we obtain the results given in Table 2.

Figures 3 and 4 show, respectively, the p.d.f.'s for the main Unitarity Triangle parameters and the selected region in the $\overline{\rho}-\overline{\eta}$ plane.

[1]In the following, for simplicity, we will denote as "direct" ("indirect") the determination of any given quantity from a direct measurement (from the UT fit without using the measurement under consideration).

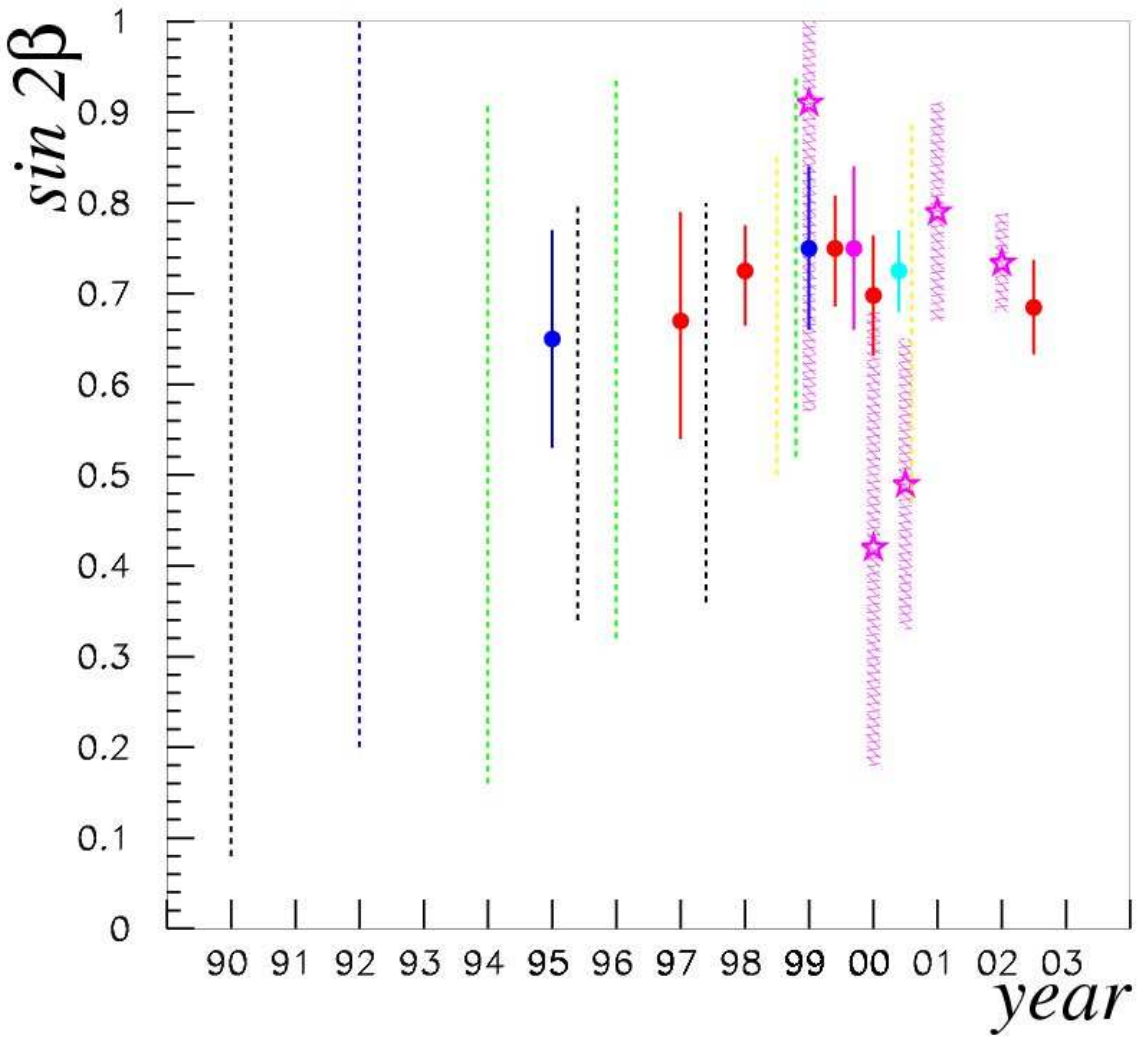

Figure 2: *Evolution of the "indirect" determination of* $\sin 2\beta$ *over the years (until 2003). From left to right, they correspond to the following papers [3, 7]: DDGN90, LMMR92, AL94, CFMRS95, BBL95, AL96, PPRS97, BF97, BPS98, PS98, AL99, CFGLM99, CPRS99, M99, CDFLMPRS00, B.et.al.00, HLLL00 and CFLPSS [2]. The dotted lines correspond to the 95% C.L. regions (the only information given in those papers). The larger bands (from year '99) correspond to values of* $\sin 2\beta$ *from direct measurements* ($\pm 1\sigma$).

3.3 Determination of other important quantities

In the previous sections we have shown that it is possible to obtain the p.d.f.'s for all the various UT parameters. It is instructive to remove from the fitting procedure the external information on the value of one (or more) of the constraints.

In this section we study the distributions of Δm_s and of the hadronic parameters. For instance, in the case of the hadronic parameters, it is interesting to remove from the fit the constraints on their values coming from lattice calculations and use them as one of

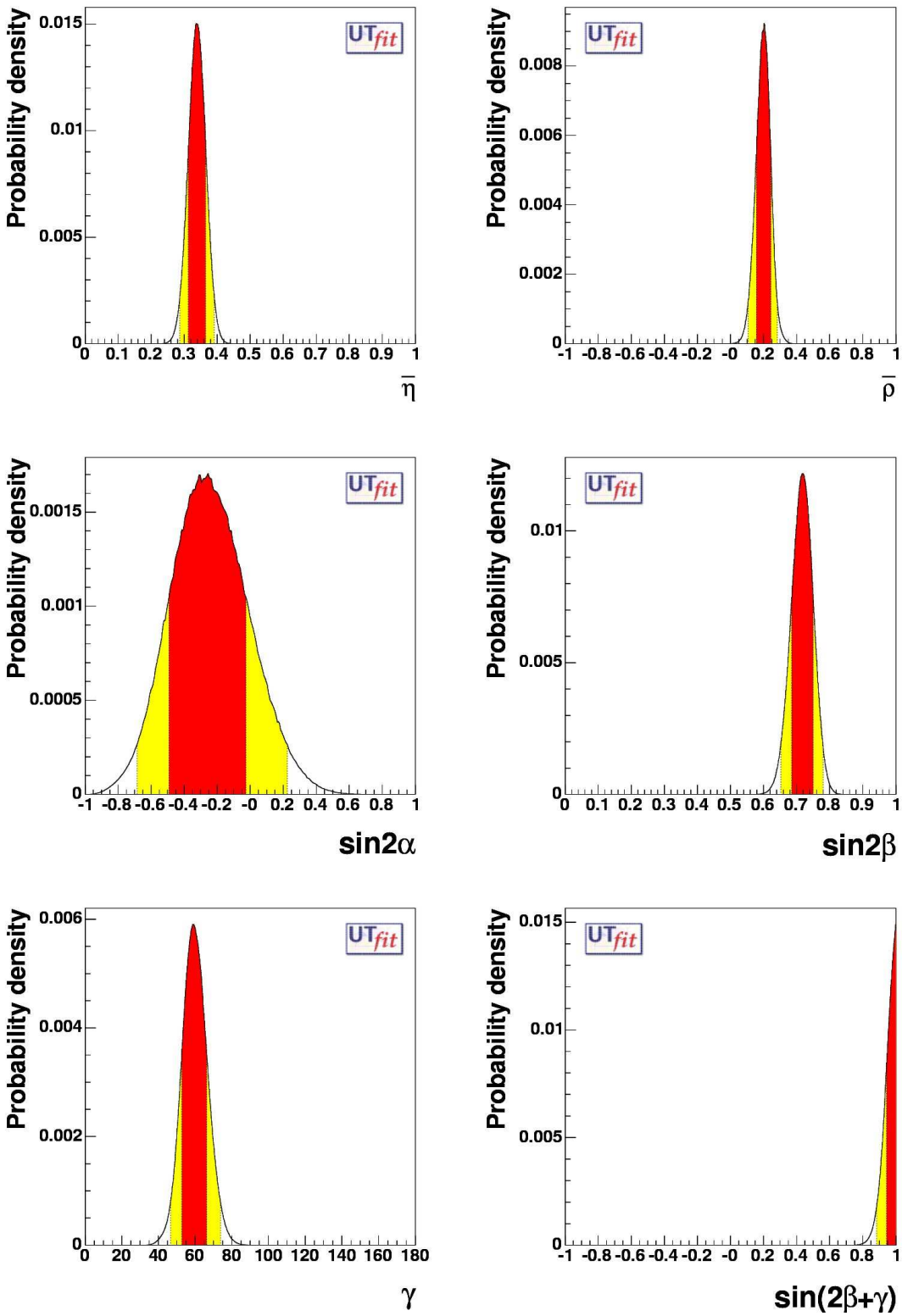

Figure 3: *From top left to bottom, the p.d.f.'s for* $\overline{\eta}$, $\overline{\rho}$, $\sin 2\alpha$, $\sin 2\beta$, γ *and* $\sin(2\beta+\gamma)$. *The red (darker) and the yellow (lighter) zones correspond respectively to 68% and 95% of the normalised area. The following contraints have been used:* $|V_{ub}|/|V_{cb}|$, ε_K, Δm_d, Δm_s *and* $\sin 2\beta$ *from the measurement of the CP asymmetry in the* $J/\psi K^0$ *decays.*

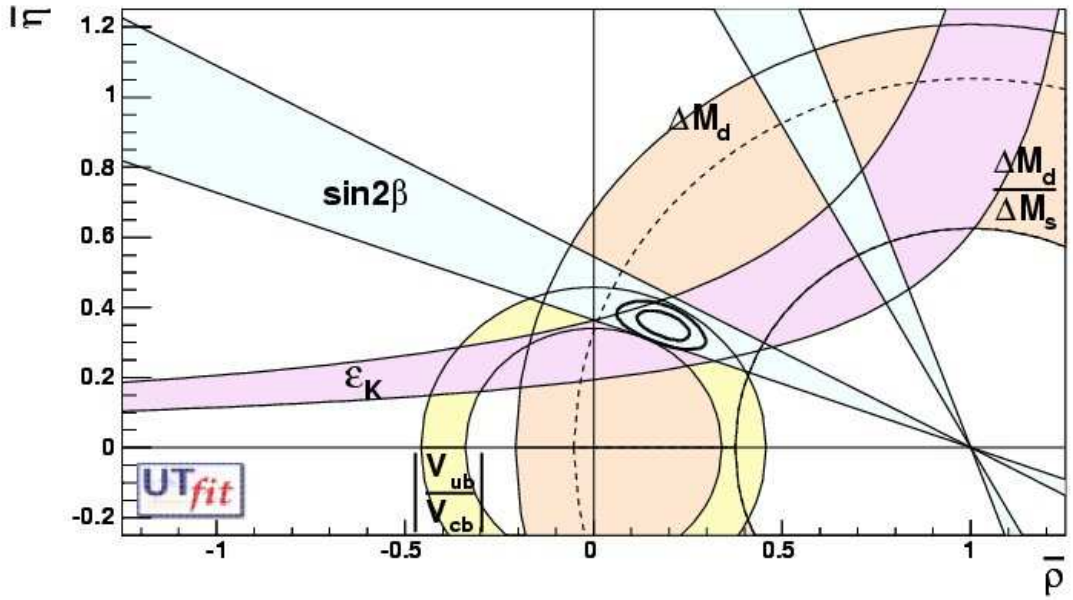

Figure 4: *Allowed regions for $\overline{\rho}$ and $\overline{\eta}$ using the parameters listed in Table 1. The closed contours at 68% and 95% probability are shown. The full lines correspond to 95% probability regions for the constraints, given by the measurements of $|V_{ub}|/|V_{cb}|$, ε_K, Δm_d, Δm_s and $\sin 2\beta$ from the measurement of the CP asymmetry in the $J/\psi K^0$ decays.*

the free parameters of the fit. In this way we may compare the uncertainty obtained on a given quantity through the UT fit to the present theoretical error on the same quantity.

3.3.1 The expected distribution for Δm_s

Removing the constraint coming from Δm_s, the probability distribution for Δm_s itself can be extracted as shown in Figure 5. The results of this exercise are given in Table 3. Present analyses at LEP/SLD have established a sensitivity of 18.3 ps^{-1} and they show a higher probability region for a positive signal (see left plot in Fig. 5: a "signal bump" appears around 17.5 ps^{-1}) well compatible with the range of the Δm_s distribution from the UT fit (see right plot in Fig. 5). Accurate measurements of Δm_s are expected from the TeVatron in the next future.

3.3.2 Determination of $f_{B_s}\sqrt{\hat{B}_{B_s}}$, $\hat{B}_K$ and ξ

To obtain the p.d.f. for a given quantity, we perform the UT fit imposing as input a uniform distribution of the quantity itself in a range much wider than the expected interval of values assumed by the parameter. Table 4 shows the results of the UT fit when one parameter at the time is taken out of the fit with this procedure (see Figure 6). The central value and the error of each of these quantities has to be compared to the current evaluation from lattice QCD, given in Table 1.

Some conclusions can be drawn. The precision on $f_{B_s}\sqrt{\hat{B}_{B_s}}$ obtained from the fit has an accuracy which is better than the current evaluation from lattice QCD. This proves

Parameter	68%	95%	99%
$\overline{\eta}$	0.348 ± 0.028	[0.293;0.403]	[0.275;0.418]
$\overline{\rho}$	0.172 ± 0.047	[0.082;0.270]	[0.051;0.302]
$\sin 2\beta$	0.725 ± 0.033	[0.645;0.772]	[0.627;0.793]
$\sin 2\alpha$	-0.16 ± 0.26	[-0.62;0.35]	[-0.75;0.48]
$\gamma[^\circ]$	61.5 ± 7.0	[47.5;76.6]	[43.3;81.6]
$\sin(2\beta+\gamma)$	> 0.94	> 0.88	> 0.84
$Im\lambda_t[10^{-5}]$	13.5 ± 1.0	[11.5;15.3]	[10.8;15.9]

Table 2: *Values and probability ranges for the Unitarity Triangle parameters obtained by using the following constraints:* $|V_{ub}|\,/\,|V_{cb}|$, Δm_d, $\Delta m_s/\Delta m_d$, ε_K *and* $\sin 2\beta$.

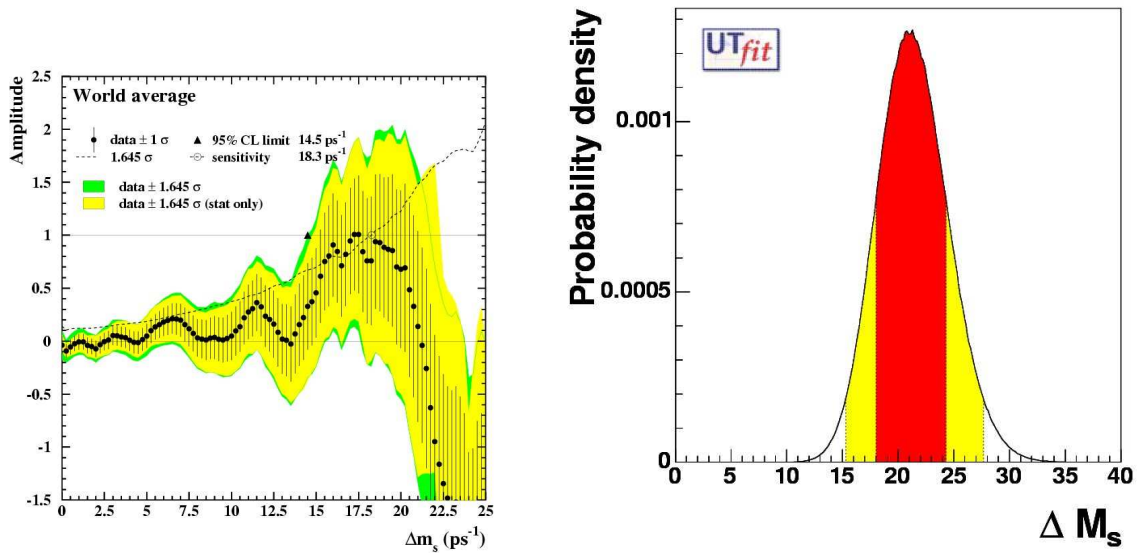

Figure 5: *Left plot: combined results [4] from all analyses on the oscillation amplitude, as a function of* Δm_s. *The points with error bars are the data; the lines show the 95% C.L. curves (in dark the systematics have been included). The dotted curve corresponds to the sensitivity. Right plot:* Δm_s *probability distributions, obtained without using the information from* $\mathrm{B}_s^0 - \overline{\mathrm{B}_s^0}$ *mixing.*

that the standard CKM fit is, in practice, weakly dependent on the assumed theoretical uncertainty on $f_{B_s}\sqrt{\hat{B}_{B_s}}$.

The result on $\hat{B}_K$ indicates that values of $\hat{B}_K$ smaller than 0.45 are excluded at 99% probability, while large values of $\hat{B}_K$ are compatible with the prediction coming from the UT fit using the other constraints. The present estimate of $\hat{B}_K$ from lattice QCD, which has a 15% relative error (Table 1), is still more precise than the indirect determination from the UT fit. Likewise, the present best determination of the parameter ξ comes from lattice QCD.

Parameter	68%	95%	99%
Δm_s(including Δm_s) [ps^{-1}]	18.3 ± 1.6	(15.4-23.1)	(15.1-27.0)
Δm_s(without Δm_s) [ps^{-1}]	21.1 ± 3.1	(15.3-27.7)	(13.7-29.9)

Table 3: *Central values and ranges for Δm_s corresponding to defined levels of probability, obtained by including or not including the information from the experimental amplitude spectrum $\mathcal{A}(\Delta m_s)$.*

Parameter	68%	95%	99%
ξ	$1.13^{+0.12}_{-0.09}$	[0.95;1.41]	[0.92;1.57]
$f_{B_s}\sqrt{\hat{B}_{B_s}}$(MeV)	263 ± 14	[236;290]	[231;320]
$\hat{B}_K$	0.65 ± 0.10	[0.49;0.87]	[0.45;0.99]

Table 4: *Values and probability ranges for the non-perturbative QCD parameters, if the external information (input) coming from the theoretical calculation of these parameters is not used in the CKM fits.*

In the above exercise we have removed from the UT fit individual quantities one by one. It is also interesting to see what can be obtained taking out two of them simultaneously. Figures 6 show the regions selected in the planes ($f_{B_s}\sqrt{\hat{B}_{B_s}}$, $\hat{B}_K$), (ξ, $\hat{B}_K$) and ($f_{B_s}\sqrt{\hat{B}_{B_s}}$, ξ). The corresponding results are summarized in Table 5.

Parameter	68%	95%	99%
$f_{B_s}\sqrt{\hat{B}_{B_s}}$(MeV)	252 ± 13	[228;283]	[219;325]
$\hat{B}_K$	0.63± 0.10	[0.48;0.87]	[0.44;1.02]
$f_{B_s}\sqrt{\hat{B}_{B_s}}$(MeV)	-	> 0.23	> 0.22
ξ	-	> 0.98	> 0.92
$\hat{B}_K$	$0.53^{+0.19}_{-0.07}$	[0.41,0.99]	[0.39,1.18]
ξ	1.33 ± 0.20	[0.99,1.63]	[0.95,1.70]

Table 5: *Values and probability ranges for the non-perturbative QCD parameters, if two external pieces of information (inputs) coming from the theoretical calculation of these parameters are not used in the CKM fits.*

4 New Constraints from UT angle measurements

The values for $\sin 2\alpha$, γ, and $\sin(2\beta+\gamma)$ given in Table 2 have to be taken as predictions for future measurements. A strong message is given for instance for the angle γ. Its indirect determination is known with an accuracy of about 10%. It has to be stressed

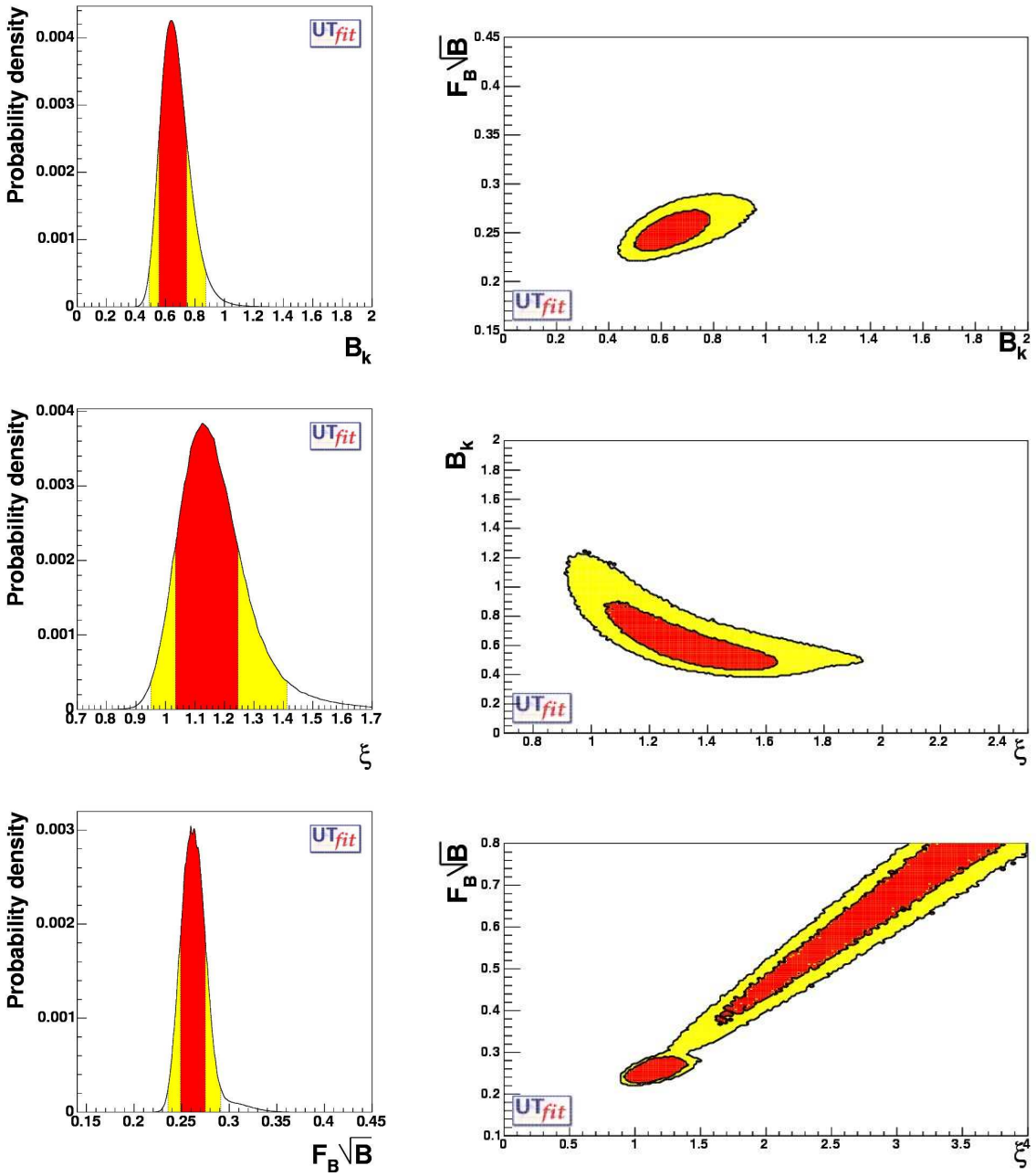

Figure 6: *One- and two-dimensional 68% and 95% probability distributions for* $\hat{B}_K$, ξ *and* $f_{B_s}\sqrt{\hat{B}_{B_s}}$ *(see Sec. 3.3.2).*

that, with present measurements, the probability for γ to be greater than 90° is only 0.0055%.

Thank to the huge statistics collected at the B-Factories, new CP-violating quantities have been recently measured allowing for the direct determination of $\sin 2\alpha$, γ, and $\sin(2\beta+\gamma)$. In the following we present the UT fit results including these new measurements and their impact on the $\overline{\rho}-\overline{\eta}$ plane.

4.1 Determination of the angle γ using DK events

Various methods using $B \to DK$ decays have been used to determine the Unitarity Triangle angle γ [8]. The basic idea in these methods is the following. A charged B^- can decay into a $D^0(\overline{D}^0)K^-$ final state via a $V_{cb}(V_{ub})$ mediated process. CP violation occurs if the D^0 and the $\overline{D}^0$ decay in the same final state. The measurement of the direct CP violation is thus sensitive to the V_{ub} and V_{cb} phase difference, γ. The same argument can be applied to $B \to D^*K$ decays.
The most important aspect of these decays is that they proceed only via tree-level diagrams, implying that the determination of γ is not affected by possible New Physics loop contributions.

One of these methods is the "GLW method" and it consists in reconstructing D^0 mesons in a specific CP (even/odd) mode. The "ADS method" is, instead, based on the fact that $D^0(\overline{D}^0)$ decays can reach the same final state through Doubly Cabibbo Suppressed (DCS) (Cabibbo Allowed (CA)) processes. The following observables are defined in these two methods:

$$\begin{aligned} R_{CP+} &= 1 + r_B^2 - 2r_B \sin\gamma \sin\delta_B \\ R_{CP-} &= 1 + r_B^2 - 2r_B \sin\gamma \cos\delta_B \\ A_{CP+} &= 2r_B \sin\gamma \sin\delta_B / R_{CP+} \\ A_{CP-} &= -2r_B \sin\gamma \sin\delta_B / R_{CP-} \\ R_{ADS} &= r_{DCS}^2 + r_B^2 + 2r_B r_{DCS} \cos\gamma \cos(\delta_B + \delta_D) \end{aligned} \tag{4}$$

where

$$r_B = \frac{\mathcal{A}(B^- \to D^0 K^-)}{\mathcal{A}(B^- \to \overline{D}^0 K^-)}, \tag{5}$$

$r_{DCS} = \sqrt{\frac{D^0 \to K^+\pi^-}{D^0 \to K^-\pi^+}}$ and δ_B (δ_D) is the difference between the strong phases of the two amplitudes in the B system (B and D systems).
In [9] a new method based on the Dalitz analysis of three-body decays has been proposed and recent results using this new technique applied to the $D^0 \to K_s\pi^-\pi^+$ decays have been published by the Belle Collaboration [10]. The advantage of this method is that the full sub-resonance structure of the three-body decay is considered, including interferences such as those used for GLW and ADS methods plus additional interferences because of the overlap of broad resonances in certain regions of the Dalitz plot. The same analysis can also be performed using $B \to D^{*0}K$ decays. The technique is identical to the one used in $B \to D^0K$ decays but the values for r_B and δ_B are different so they will be indicated as r_B^* and δ_B^* in the following. It is also interesting to note that the Dalitz analysis has only a two-fold discrete ambiguity ($\gamma+\pi, \gamma-\pi$) and not a four-fold ambiguity as in case of the GLW and ADS methods. It has to be noted that experimental likelihoods have been

used to correctly implement the measurement of R_{ADS} and the Dalitz result.
A summary of the experimental results is given in Table 6.

Observable	World Average
A_{CP+}	0.07 ± 0.13
A_{CP-}	-0.19 ± 0.18
R_{CP+}	1.09 ± 0.16
R_{CP-}	1.30 ± 0.25
R_{ADS}	0.0054 ± 0.0124
$r_B(r_B^*)$	$0.26^{+0.10}_{-0.14} \pm 0.03 \pm 0.04$ $(0.20^{+0.19}_{-0.17} \pm 0.02 \pm 0.04)$
γ	$77^{+19}_{-17} \pm 13 \pm 11$ (Belle Dalitz)

Table 6: *Summary of the results obtained with $B \to D^{(*)}K$ decays and using the GLW and the ADS methods. The last two lines give the results from the Dalitz analysis [9], for which the ambiguity $\gamma \to \pi - \gamma$ is implicit.*

All measurements in Table 6 are used to extract γ. The p.d.f.'s of γ, r_B (r_B^*) and the selected region in the γ vs r_B plane are shown in Figure 7, where also the effect of this measurement in the $\overline{\rho} - \overline{\eta}$ plane is shown.

The comparison between the direct and the indirect determination is:

$$\begin{aligned} \gamma[^\circ] &= 61.5 \pm 7.0\ [47.5; 76.6] \text{ at } 95\%\ C.L.\ \text{indirect} \\ \gamma[^\circ] &= 73 \pm 27\ [4; 133]\ \text{ at } 95\%\ C.L. (-107 \pm 27\ \ [-176; -47])\ \text{direct} \end{aligned} \tag{6}$$

An important result of this analysis is also the p.d.f. for r_B from which the following result can be given:

$$r_B = 0.105 \pm 0.065\ [\ <\ 0.22] \text{ at } 95\%\ C.L.\ \text{direct from DK.} \tag{7}$$

4.2 Determination of sin2α using $\pi\pi$ and $\rho\rho$ events

In the absence of contributions from penguin diagrams, the measurements of the parameter S of the time-dependent CP asymmetry for $B^0 \to \pi^+\pi^-$ and $B^0 \to \rho^+\rho^-$ give measurements of the quantity $\sin(2\alpha)$. Even in presence of penguins, one can use the SU(2) flavour symmetry to connect the measured value of S$\equiv \sin(2\alpha_{eff})$ to the value of $\sin(2\alpha)$, constraining the contribution from penguin diagrams using the Branching Fractions and the direct CP asymmetry measurements of all the $B \to \pi\pi$ ($B \to \rho\rho$) decays [11]. The decay amplitudes in the $SU(2)$ limit and neglecting electroweak penguins can be written as:

$$\begin{aligned} A^{+-} &= -Te^{-i\alpha} + Pe^{i\delta_P} \\ A^{+0} &= -\frac{1}{\sqrt{2}}\left[e^{-i\alpha}(T + T_c\ e^{i\delta_{T_c}})\right] \\ A^{00} &= -\frac{1}{\sqrt{2}}\left[e^{-i\alpha}T_c\ e^{i\delta_{T_c}} + P\ e^{i\delta_P}\right]. \end{aligned} \tag{8}$$

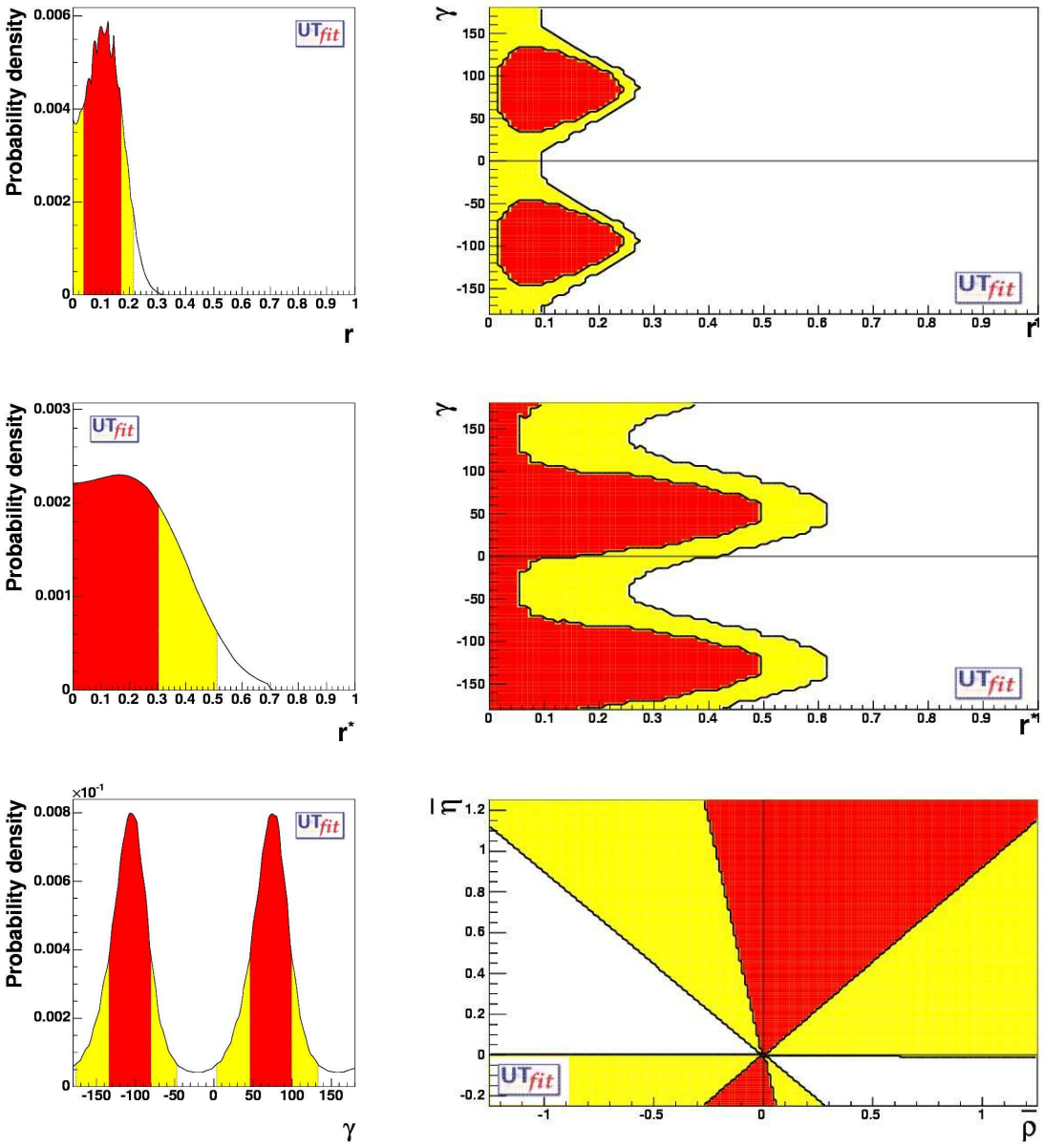

Figure 7: *P.d.f.'s for r_b from DK (top-left), for r_b^* from D^*K (center-left) and for γ (bottom-left) using the results from $B \to D^{(*)}K$ decays. The plots on the right show the measurement of the angle γ in the $r_b^{(*)} - \gamma$ (top, center) and $\overline{\rho} - \overline{\eta}$ (bottom) planes.*

They can be expressed in terms of three independent hadronic amplitudes, the absolute values of which are denoted as T, T_c and P. Similarly, δ_P and δ_{T_c} are the strong phases of P and T_c, once the phase convention is chosen so that T is real. It should be noted that these parameters are different for $B \to \pi\pi$ and $B \to \rho\rho$ decays. For the $B \to \rho\rho$ decays we have in principle to further double the parameters for the longitudinal and the transverse polarization. On the other hand the experimental measurements are compatible with decays which are fully longitudinally polarized. For this reason, in case of $B \to \rho\rho$, we make the assumption of fitting the amplitude with only one set of parameters.
Notice that the number of parameters exceeds the number of available measurements.

	$\pi\pi$			$\rho\rho$		
Observable	BaBar	Belle	Average	BaBar	Belle	Average
C	-0.19 ± 0.20	-0.58 ± 0.17	-0.46 ± 0.13	-0.23 ± 0.28		-0.23 ± 0.28
S	-0.40 ± 0.22	-1.00 ± 0.22	-0.74 ± 0.16	-0.19 ± 0.35		-0.19 ± 0.35
$BR^{+-}(10^{-6})$	4.7 ± 0.6	4.4 ± 0.7	4.6 ± 0.4	30.0 ± 6.0		30.0 ± 6.0
$BR^{+0}(10^{-6})$	5.5 ± 1.2	5.0 ± 1.3	5.2 ± 0.8	22.5 ± 8.1	31.7 ± 9.8	26.4 ± 6.4
$BR^{00}(10^{-6})$	2.1 ± 0.7	1.6 ± 0.6	1.9 ± 0.5	0.6 ± 0.8		0.6 ± 0.8

Table 7: *Experimental inputs from Isospin Analysis in $B \to \pi\pi$ and $B \to \rho\rho$ decays [4]. The $B \to \rho\rho$ decays are assumed to be fully polarized, in agreement with available measurements.*

Nevertheless, one can still extract information on α, in the same spirit of the bounds à la Grossman-Quinn.
Using the experimental measurements given in Table 7, we thus constrain all these parameters and the value of the UT angle α.

In Figure 8 we show the results in terms of $\sin 2\alpha$ and of the allowed region in the $\overline{\rho} - \overline{\eta}$ plane, from BaBar measurements only and using the world average. It has to be noted that the unphysical value found by Belle has a strong impact on the selected area. On the other hand, the leading contribution is given by $B \to \rho\rho$ decays.

The result we get can be compared to the indirect determination from the standard fit:

$$\begin{aligned}
\sin 2\alpha &= -0.16 \pm 0.26\ [-0.62; 0.35] \text{ at } 95\%\ C.L.\ \text{ indirect} \\
\sin 2\alpha &= -0.24^{(+0.19)}_{(-0.24)}\ [-0.75; 0.26] \text{ at } \ 95\%\ C.L.\ \ \pi\pi \text{ and } \rho\rho \text{ BaBar} \\
\sin 2\alpha &= -0.55^{(+0.21)}_{(-0.18)}\ [-0.94; -0.21] \text{ at } \ 95\%\ C.L.\ \ \pi\pi \text{ and } \rho\rho \text{ (WA)}. \qquad (9)
\end{aligned}$$

It is important to stress the fact that the main assumptions we are using here, i.e. the validity of SU(2) flavour symmetry and the absence of E.W. penguins. can be directly tested in this framework comparing the experimental and the fitted values of the Branching Fractions (see Table 8). It is clear that all experimental measurements of $B \to \pi\pi$ are in agreement with the SU(2) assumption. On the contrary, we observe from Table 8 a disagreement between the fitted and the experimental value of $BR(B^+ \to \rho^+\rho^0)$. This discrepancy is shown in Figure 9 and, if confirmed with increased accuracy, it would point towards a violation of the assumptions on which the parameterization of eqs. (8) is based.

	$\pi\pi$		$\rho\rho$	
Observable	Average	UTfit	Average	UTfit
$BR^{+-}(10^{-6})$	4.6 ± 0.4	4.6 ± 0.4	30.0 ± 6.0	32.1 ± 5.5
$BR^{+0}(10^{-6})$	5.2 ± 0.8	5.2 ± 0.8	26.4 ± 6.4	20.5 ± 4.8
$BR^{00}(10^{-6})$	1.9 ± 0.5	1.8 ± 0.5	0.6 ± 0.8	0.7 ± 0.8

Table 8: *Comparison of input and output values for the Branching Fractions of $B \to \pi\pi$ and $B \to \rho\rho$ decay modes.*

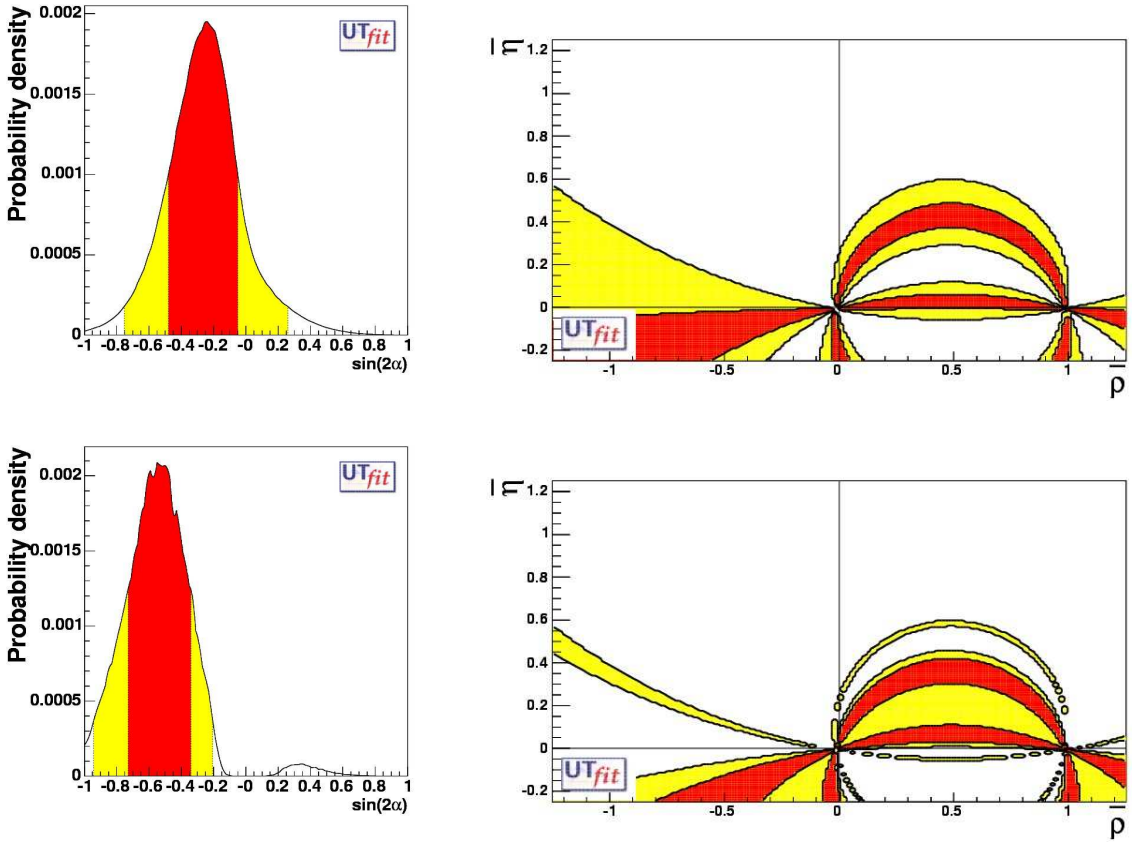

Figure 8: *Distribution of sin(2α) (left) and relative bound on* $\overline{\rho} - \overline{\eta}$ *plane (right), using BaBar only (top) and World Average (bottom) [4] values.*

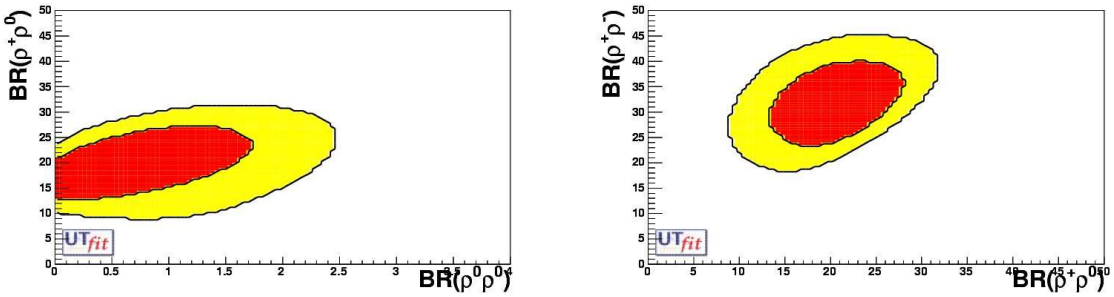

Figure 9: *Plots showing the correlation of* $BR(B^+ \to \rho^+\rho^0)$ *vs* $BR(B^0 \to \rho^0\rho^0)$*(left) and* $BR(B^0 \to \rho^+\rho^-)$ *vs* $BR(B^+ \to \rho^+\rho^0)$*(right) as obtained from SU(2) parameterizations in UTfit.*

4.3 Determination of $\sin(2\beta + \gamma)$ using $D^{(*)}\pi$ events

$\sin(2\beta+\gamma)$ can be extracted from time-dependent asymmetries in B decays to $D^{(*)}$ π final states, looking at the interference effects between the decay amplitudes implying $b \to c$

and $b \to u$ transitions. The time-dependent rates can be written as:

$$\begin{aligned} R(B^0 \to D^{(*)-}\pi^+) &= N\ e^{-\Gamma t}\ (1 + C\ \cos(\Delta m_d t) + S\ \sin(\Delta m_d t)\ ) \\ R(\overline{B}^0 \to D^{(*)-}\pi^+) &= N\ e^{-\Gamma t}\ (1 - C\ \cos(\Delta m_d t) - S\ \sin(\Delta m_d t)\ ) \\ R(B^0 \to D^{(*)+}\pi^-) &= N\ e^{-\Gamma t}\ (1 + C\ \cos(\Delta m_d t) - \overline{S}\ \sin(\Delta m_d t)\ ) \\ R(\overline{B}^0 \to D^{(*)+}\pi^-) &= N\ e^{-\Gamma t}\ (1 - C\ \cos(\Delta m_d t) + \overline{S}\ \sin(\Delta m_d t)\ ) \end{aligned} \tag{10}$$

where S and C parameters are defined as

$$\begin{aligned} S &= 2\ r/(1+r^2)\sin(2\beta+\gamma-\delta) \\ \overline{S} &= 2\ r/(1+r^2)\sin(2\beta+\gamma+\delta) \\ C &= (1-r^2)/(1+r^2) \end{aligned} \tag{11}$$

and r and δ are the absolute value and the phase of the amplitude ratio $A(\overline{B}^0 \to D^-\pi^+)/A(B^0 \to D^-\pi^+)$. This ratio r is rather small being of the order of $|V_{ub}/V_{cb}| \simeq 0.02$.

There is a correlation between the tag side and the reconstruction side in time dependent CP measurements at B-Factories [12]. This is related to the fact that interference between $b \to c$ and $b \to u$ transitions in $B \to DX$ decays can occur also in the tag side. S and $\overline{S}$ entering the time dependent rates can be replaced by

$$\begin{aligned} a &= 2r\sin(2\beta+\gamma)\cos(\delta) \\ b &= 2r^{'}\sin(2\beta+\gamma)\cos(\delta^{'}) \\ c &= 2\cos(2\beta+\gamma)(r\sin(\delta) - r^{'}\sin(\delta^{'})) \end{aligned} \tag{12}$$

where $r^{'}$ and $\delta^{'}$ are the analogue of r and δ for the tag side. It is important to stress that this interference on the tag side cannot occur when B mesons are tagged using semileptonic decays. In other words, $r^{'} = 0$ when only semileptonic decays are considered. In the following we will consider the observables a, c(lepton), a^* and c^*(lepton), which are functions of $r^{(*)}$, $\delta^{(*)}$ and $2\beta+\gamma$.

BaBar and Belle provided three different measurements of this channel, with total (both) [13] or partial (BaBar only) [14] reconstruction of the final state, as summarized in Table 9.

Parameters	HFAG average [4]
a	-0.038 ± 0.021
a*	0.012 ± 0.030
c (lepton)	-0.041 ± 0.029
c* (lepton)	-0.015 ± 0.044

Table 9: *Summary of the experimental results from BaBar and Belle, as reported in [4].*

We use directly the four experimental quantities: $a^{(*)}$ and $c^{(*)}$(lepton) defined before and we build a global p.d.f. as the product of the p.d.f.'s of these four quantities. We do not make any assumption on r and r^* which are extracted in the range [0.0,0.1]. The

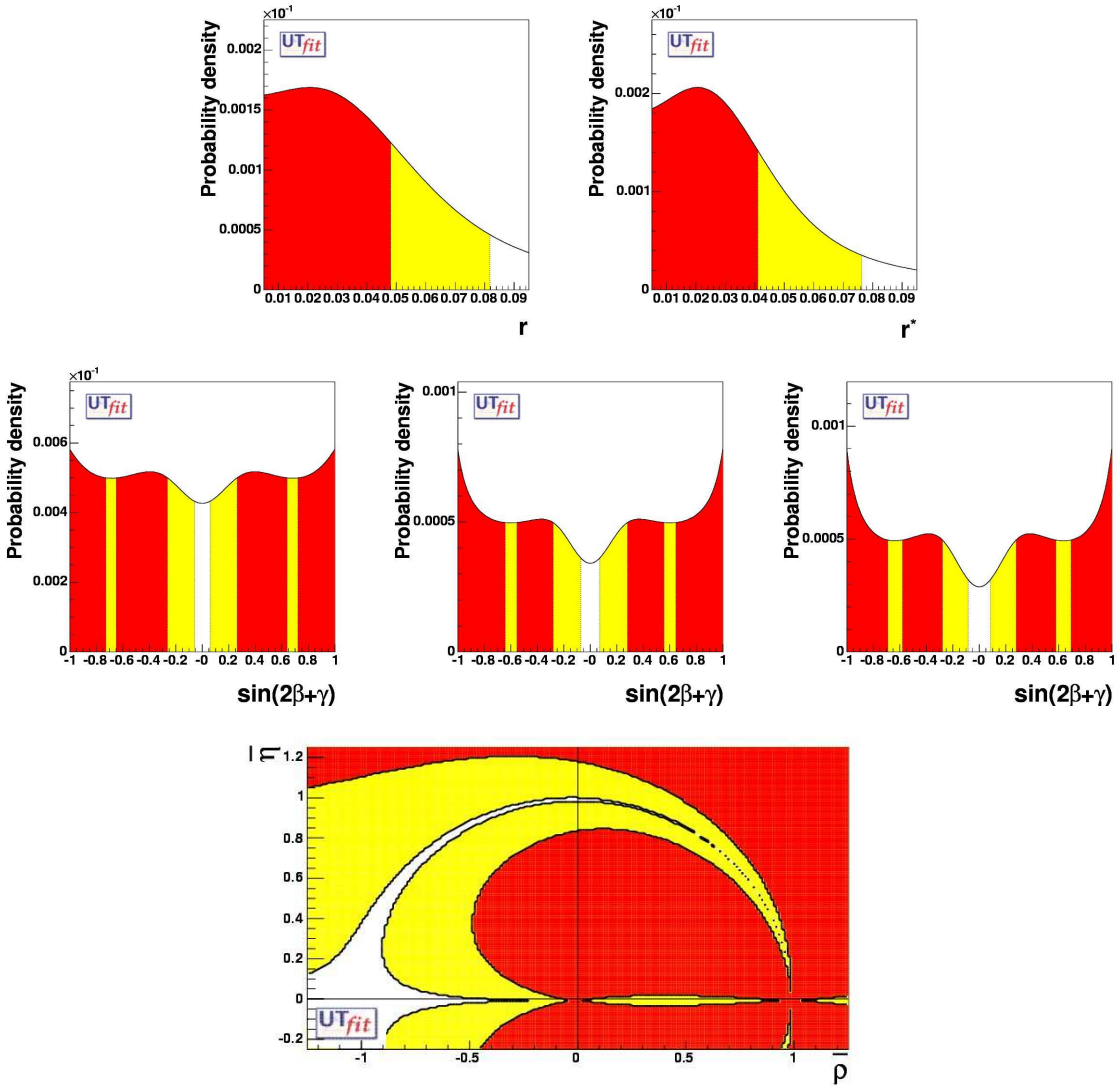

Figure 10: *Distributions for r for $D\pi$ (top-left), r^* for $D^*\pi$ (top-right),* $\sin(2\beta+\gamma)$ *for $D\pi$ (middle-left),* $\sin(2\beta+\gamma)$ *for $D^*\pi$ (middle-center) and* $\sin(2\beta+\gamma)$ *combined (middle-right) and bound from* $\sin(2\beta+\gamma)$ *on the $\overline{\rho}-\overline{\eta}$ plane (bottom).*

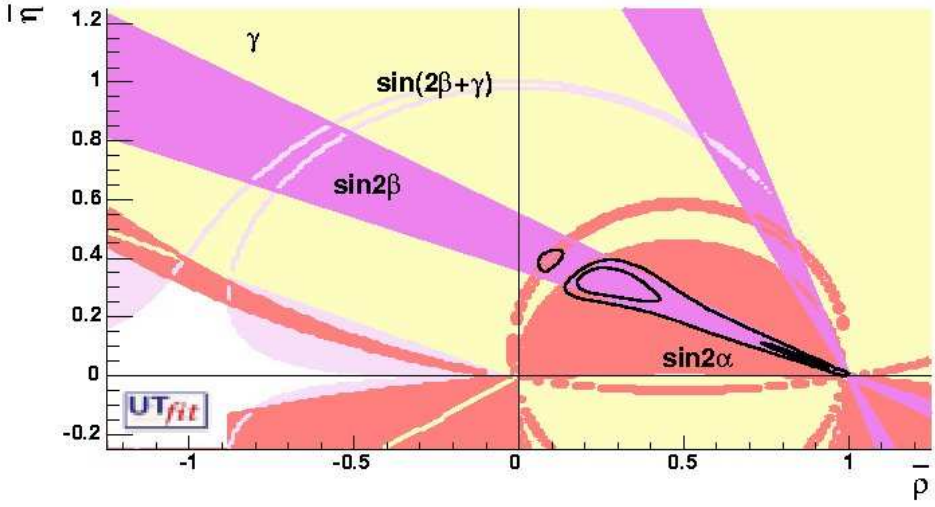

Figure 11: *Allowed regions for $\overline{\rho}$ and $\overline{\eta}$ obtained using the measurements of the UT angles in the B sector:* $\sin 2\beta$, $\sin 2\alpha$, $\sin(2\beta+\gamma)$ *and* γ. *The closed contours at* 68% *and* 95% *probability are shown. The full zones correspond to* 95% *probability regions from individual constraints.*

results on r, r^*, $\sin(2\beta+\gamma)$ and the impact of this measurement in the $\overline{\rho}-\overline{\eta}$ plane are shown in Figure 10.

The comparison between the direct and the indirect determination of $\sin(2\beta+\gamma)$ is given below:

$$\begin{array}{lcll} \sin(2\beta+\gamma) & > & 0.94 \text{ at } 68\% \ C.L. (> 0.88 \text{ at } 95\% \ C.L.) & \text{indirect} \\ \sin(2\beta+\gamma) & > & 0.28 \text{ at } 68\% \ C.L. (> 0.08 \text{ at } 95\% \ C.L.) & \mathrm{D}^{(*)}\pi. \end{array} \quad (13)$$

4.4 Determination of the Unitarity Triangle parameters using also the new UT angle measurements

It is interesting to see the selected region in $\overline{\rho}-\overline{\eta}$ plane from the measurements of the UT angles in the B sector. The plot is shown in Figure 11. In Table 10 we report the results we get using these constraints.

The results given in Table 11 are obtained using all the available constraints: $|V_{ub}|/|V_{cb}|$, Δm_d, $\Delta m_s/\Delta m_d$, ε_K, $\sin 2\beta$, γ, $\sin(2\beta+\gamma)$ and $\sin 2\alpha$. Figure 12 shows the corresponding selected region in the $\overline{\rho}-\overline{\eta}$ plane.

5 Compatibility plots, or how to discover New Physics in the flavour sector

In this section we discuss the interest of measuring the various physical quantities entering the UT analysis with a better precision. We investigate, in particular, to which extent future and improved determinations of the experimental constraints, such as $\sin 2\beta$, Δm_s

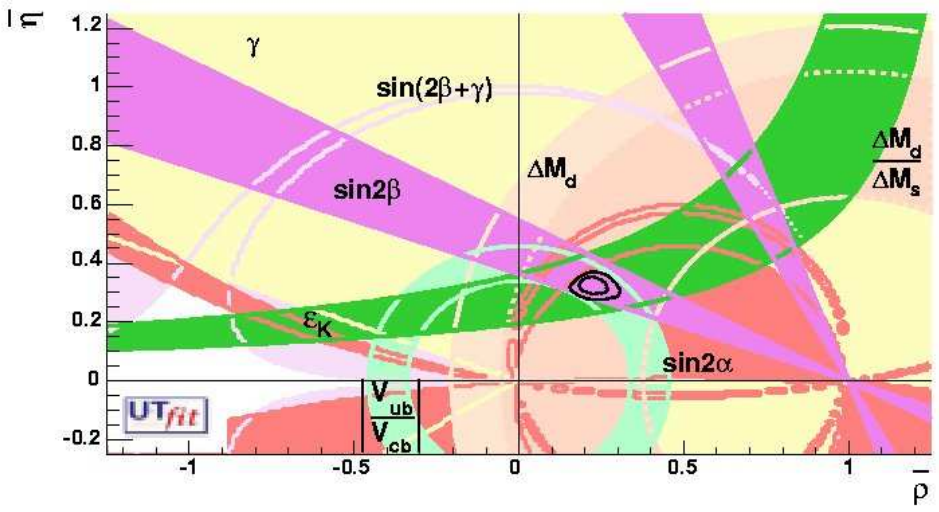

Figure 12: *Allowed regions for* $\overline{\rho}$ *and* $\overline{\eta}$ *using the parameters listed in Table 1. The closed contours at* 68% *and* 95% *probability are shown. The full lines correspond to* 95% *probability regions for the constraints, given by the measurements of* $|V_{ub}|$ / $|V_{cb}|$, ε_K, Δm_d, Δm_s *and* $\sin 2\beta$,γ, $\sin(2\beta+\gamma)$ *and* $\sin 2\alpha$.

Parameter	68%	95%	99%
$\overline{\eta}$	$0.265^{+0.120}_{-0.070}$	[0.165;0.869]	[0.052;0.980]
$\overline{\rho}$	$0.315^{+0.40}_{-0.51}$	[0.040;0.378]	[0.004;0.437]
$\sin 2\beta$	0.733 ± 0.049	[0.636;0.828]	[0.606;0.858]
$\sin 2\alpha$	-0.66 ± 0.26	<0.48	<0.59
$\gamma[^\circ]$	$50.0^{+9.2}_{-14.9}$	<61.5	<79.6
$Im\lambda_t[10^{-5}]$	12.1 ± 1.6	[5.8,14.3]	[5.1,16.0]

Table 10: *Values and probability ranges for the Unitarity Triangle parameters obtained by using* $\sin 2\beta$, γ, $\sin(2\beta+\gamma)$ *and* $\sin 2\alpha$.

and γ, could allow us to possibly invalidate the SM, thus signaling the presence of NP effects.

5.1 Compatibility between individual constraints. The pull distributions.

In CKM fits based on a χ^2 minimization, a conventional evaluation of compatibility stems automatically from the value of the χ^2 at its minimum. The compatibility between constraints in the Bayesian approach is simply done by comparing two different p.d.f.'s. For example, compare the value for $\sin 2\beta$ obtained from the measurement of the sides of the Unitarity Triangle (the random variable $\mathbf{x_1}$) with the one obtained from the direct measurement of the CP violation asymmetry (the random variable $\mathbf{x_2}$). In this case the

Parameter	68%	95%	99%
$\overline{\eta}$	0.324 ± 0.020	[0.283,0.359]	[0.268,0.373]
$\overline{\rho}$	0.225 ± 0.030	[0.171,0.288]	[0.151,0.326]
$\sin 2\beta$	0.710 ± 0.032	[0.645,0.773]	[0.624,0.792]
$\sin 2\alpha$	$-0.44^{+0.17}_{-0.09}$	[-0.68,-0.18]	[-0.81,-0.13]
$\gamma[^\circ]$	$53.9^{+5.5}_{-2.4}$	[46.6,62.4]	[41.1,64.6]
Im $\lambda_t[10^{-5}]$	12.4 ± 0.8	[11.0,14.0]	[10.5,14.5]

Table 11: *Values and probability ranges for the Unitarity Triangle parameters obtained by using all the available constraints:* $|V_{ub}|\,/\,|V_{cb}|$, Δm_d, $\Delta m_s/\Delta m_d$, ε_K *and* $\sin 2\beta$, γ, $\sin(2\beta+\gamma)$ *and* $\sin 2\alpha$.

distribution of the random variable $\mathbf{y} = \mathbf{x_1} - \mathbf{x_2}$ has to be constructed and the integral of this distribution above (or below) zero gives the one side probability of compatibility[2]. The advantage of this approach is that the full overlap between the p.d.f.'s is evaluated instead of a single number.
If two constraints turn out to be incompatible, further investigation is necessary to tell if this originates from a "wrong" evaluation of the input parameters or from a New Physics contribution.

5.2 Pull distribution for $\sin 2\beta$. Role of $\sin 2\beta$ from Penguin processes.

We start this analysis by considering the measurement of sin2β. The plots in Figure 13 show the compatibility ("pull") between the direct and indirect distributions of $\sin 2\beta$, in the SM, as a function of the measured value (x-axis) and error (y-axis) of $\sin 2\beta$.

¿From the left plot in Figure 13, it can be seen that, considering the actual precision of about 0.05 on the measured value of $\sin 2\beta$, the 3σ compatibility region is between [0.49-0.87]. Values outside this range would be, therefore, not compatible with the SM prediction at more than 3σ level. To get these values, however, the presently measured central value should shift by more than 4σ.

The conclusion that can be derived from Figure 13 is the following: although the improvement of the error on sin2β has an important impact on the accuracy of the UT parameter determination, it is very unlikely that in the near future we will be able to use this measurement to detect any failure of the SM, unless the other constraints entering the fit improve substantially or, of course, in case the central value of the direct measurement move away from the present one by several standard deviations.

The right plot in Figure 13 shows the compatibility of the direct and indirect distributions of $\sin 2\beta$ as a function of the measured value and error of $\sin 2\beta$. The difference with respect to the left plot is that, in this case, all the available constraints have been used to obtain the indirect distribution of $\sin 2\beta$, including the direct measurement of $\sin 2\beta$

[2]In the Gaussian case it coincides with the pull which is defined as the difference between the central values of the two distributions divided by the sum in quadrature of the r.m.s of the distributions themselves.

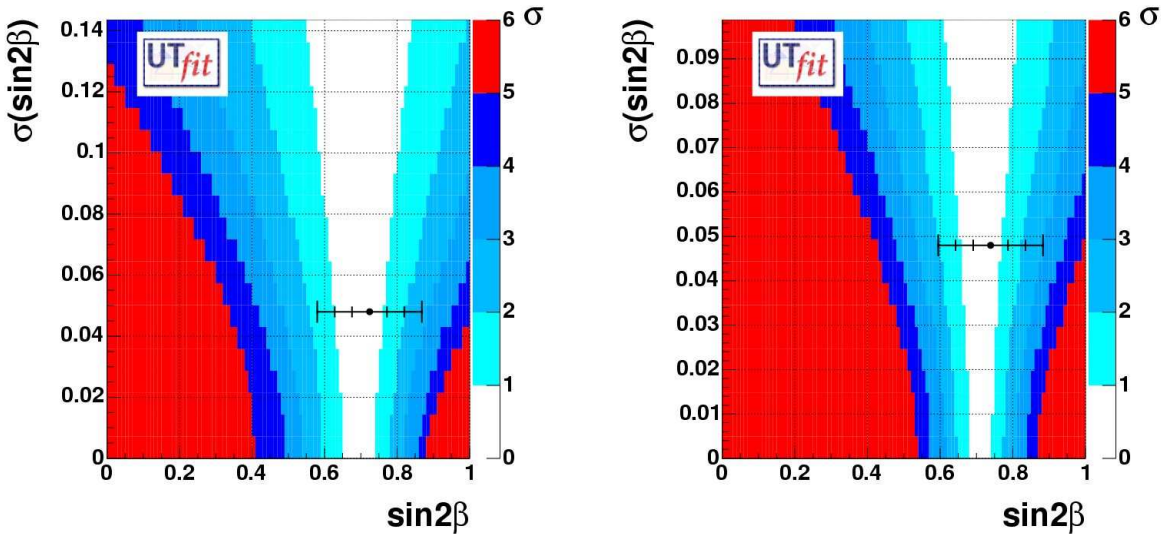

Figure 13: *The compatibility ("pull") between the direct and indirect determination of* $\sin 2\beta$ *as a function of the value and error of* $\sin 2\beta$ *measured from CP asymmetry in* $J/\psi K^0$ *decays. The indirect distribution of* $\sin 2\beta$ *is computed without using the direct measurement (left plot) or using the measurement of* $\sin 2\beta$ *from CP asymmetry in* $J/\psi K^0$ *decays (right plot). The compatibility regions from 1 to 6* σ *are also displayed.*

Observable	BaBar	Belle	Average
$S_{\phi K^0_S}$	$0.47 \pm 0.34^{+0.08}_{-0.06}$	$-0.96 \pm 0.50^{+0.09}_{-0.11}$	0.02 ± 0.29
$C_{\phi K^0_S}$	$0.01 \pm 0.33 \pm 0.10$	$0.15 \pm 0.29 \pm 0.08$	0.09 ± 023
$S_{K^0_S\pi^0}$	$0.48^{+0.38}_{-0.47} \pm 0.11$	-	$0.48^{+0.38}_{-0.47} \pm 0.11$
$C_{K^0_S\pi^0}$	$0.40^{+0.27}_{-0.28} \pm 0.10$	-	$0.40^{+0.27}_{-0.28} \pm 0.10$

Table 12: *Experimental inputs for S and C in* $B^0 \to \phi K^0_S$ *and* $B^0 \to K^0_S\pi^0$ *decays [4].*

from $J/\psi K^0$.

It was pointed out some time ago that the comparison of the time-dependent CP asymmetries in various B decay modes could provide evidence of NP in B decay amplitudes [15]. Since $\sin 2\beta$ is known from $J/\psi K^0$, a significant deviation of the time-dependent asymmetry parameters of penguin dominated channels $B^0 \to \phi K^0$ and $B^0 \to K^0\pi^0$ from their expected values would indicate the presence of NP.

These asymmetries have been recently measured at B-Factories [16] and are reported in Table 12.

In a naïve approach, one expects S $\sim \sin 2\beta$ and C ~ 0, but the theoretical uncertainties related to hadronic physics can change this expectation. Starting from the value of sin2β of the standard analysis, we used the Charming Penguins model [17] to take into account these hadronic uncertainties and quantify the sensitivity of future measurements with the compatibility plots shown in Figure 14. It has to be noted that, including these hadronic uncertainties, the theoretical predictions of S and C in Table 12 have a typical uncertainty of ~ 0.09 [18].

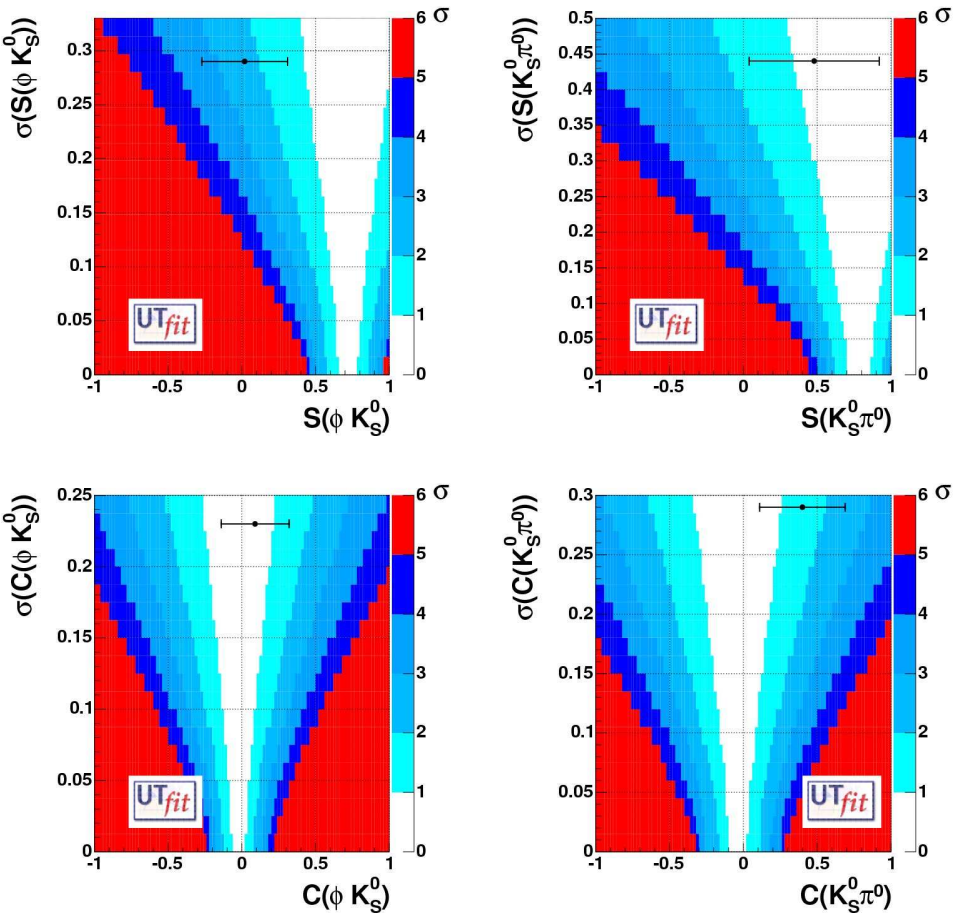

Figure 14: *Compatibility plot for S (top) and C (bottom) for ϕK_S^0 (left) and $K_S^0\pi^0$ (right), using UTfit result and Charming Penguins model. Experimental measurements are superimposed.*

5.3 Pull distribution for Δm_s

The plot in Figure 15 shows the compatibility of the indirect determination of Δm_s with a future determination of the same quantity, obtained using or ignoring the experimental information coming from the present bound.

¿From the plot in Figure 15 it can be concluded that, once a measurement of Δm_s with the expected accuracy of ~ 1 ps^{-1} is available, a value of Δm_s greater than 32 ps^{-1} would imply New Physics at 3 σ level.

5.4 Pull distribution for the angle γ

The plot in Figure 16 shows the compatibility of the indirect determination of γ with a future determination of the same angle obtained from B decays. It can be noted that even in case the angle γ can be measured with a precision of 10° from B decays, the predicted 3σ region is still rather large, corresponding to the interval [25-100]°. Values beyond 100° would clearly indicate physics beyond the Standard Model. The actual determination of the angle γ is not yet precise enough to test the validity of the Standard Model as shown

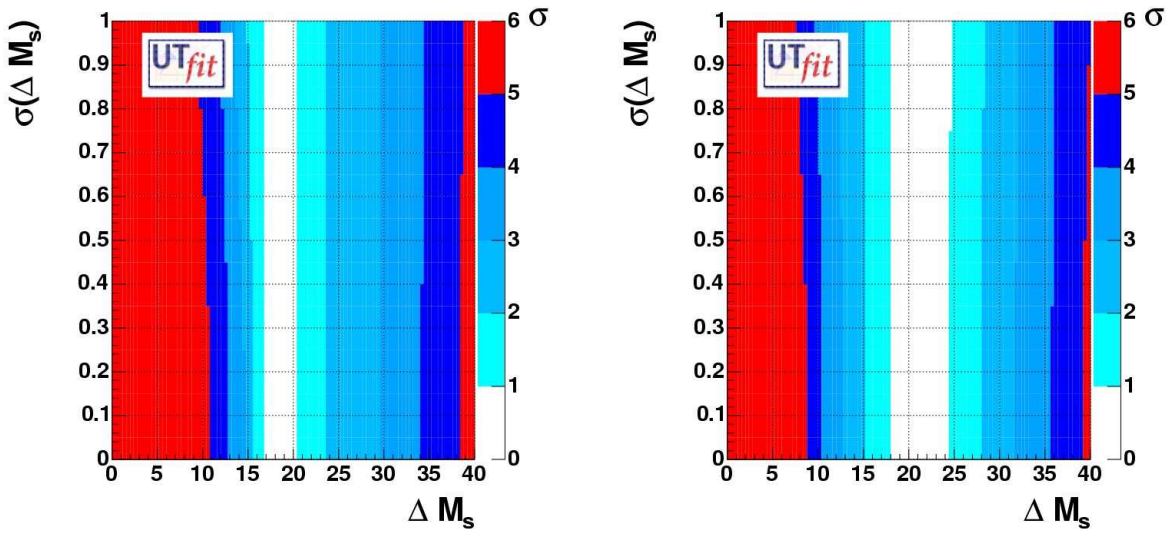

Figure 15: *The compatibility of the direct and indirect determination of Δm_s, as a function of the value of Δm_s, using (left) or ignoring (right) the present experimental bound.*

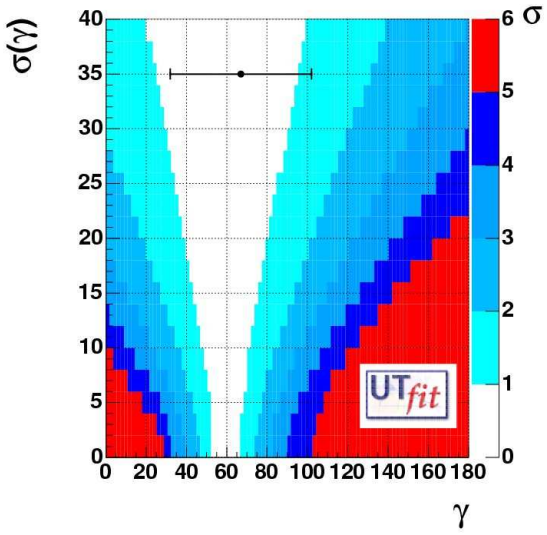

Figure 16: *The compatibility of the direct and indirect determination of γ, as a function of the value and the error of γ, using the UT fit results.*

by the point with the error bar in Figure 16 and given in equation (6). Nevertheless, a direct determination of γ is of crucial importance to test NP models [19].

6 Conclusions

Flavour physics in the quark sector has entered its mature age. Today the Unitarity Triangle parameters are known with good precision. A crucial test has been already done: the comparison between the Unitarity Triangle parameters, as determined with quantities sensitive to the sides of the triangle (semileptonic B decays and oscillations), and the measurements of CP violation in the kaon (ϵ_K) and in the B ($\sin 2\beta$) sectors. The agreement is "unfortunately" excellent. The Standard Model is "Standardissimo": it is also working in the flavour sector. This agreement is also due to the impressive improvements achieved on OPE, HQET and LQCD theories which have been used to extract the CKM parameters.

Many B decay Branching Fractions and relative CP asymmetries have been measured at B-Factories. The outstanding result is the determination of $\sin 2\beta$ from B hadronic decays into charmonium-K^0 final states. On the other hand many other exclusive hadronic rare B decays have been measured and constitute a gold mine for weak and hadronic physics, allowing in principle to extract different combinations of the Unitarity Triangle angles.

Besides presenting an update of the standard UT analysis, we have shown in this paper that new measurements at B-Factories start to have an impact on the overall picture of the Unitarity Triangle determination. In the following years they will provide further tests of the Standard Model in the flavour sector to an accuracy up to the per cent level.

Finally, introducing the compatibility plots, we have studied the impact of future measurements on testing the SM and looking for New Physics.

7 Acknowledgements

We would like to warmly thank people which provide us the experimental and theoretical inputs which are an essential part of this work and helped us with useful suggestions for the correct use of the experimental information. We thank: A. Bevan, T. Browder, C. Campagnari, G. Cavoto, M. Danielson, R. Faccini, F. Ferroni, M. Legendre, O. Long, F. Martinez, L. Roos, A. Poulenkov, M. Rama, Y. Sakai, M.-H. Schune, W. Verkerke, M. Zito. We also thank P. Gambino and A. Soni for useful discussions. Finally, we thank M. Baldessari, C. Bulfon, and all the BaBar Rome group for help in the realization and for hosting the web site.

References

[1] **UT***fit* Collaboration : M. Bona, M. Ciuchini, G. D'Agostini, E. Franco, V. Lubicz, G. Martinelli, F.Parodi, M. Pierini, P. Roudeau, C. Schiavi, L. Silvestrini, A. Stocchi. `http://www.utfit.org`

[2] M. Ciuchini, E. Franco, V. Lubicz, F. Parodi, L. Silvestrini and A. Stocchi, "Unitarity Triangle in the Standard Model and sensitivity to new physics" (hep-ph/0307195);

M. Ciuchini, G. D'Agostini, E. Franco, V. Lubicz, G. Martinelli, F. Parodi, P. Roudeau, A. Stocchi, "2000 CKM-Triangle Analysis A Critical Review with Updated Experimental Inputs and Theoretical Parameters", **JHEP 0107** (2001) 013. (hep-ph/0012308); A. J. Buras, F. Parodi, A. Stocchi, "The CKM Matrix and The Unitarity Triangle: another Look" **JHEP 0301** (2003) 029 (hep-ph/0207101).

[3] M. Lusignoli, L. Maiani, G. Martinelli and L. Reina, Nucl. Phys. B **369**, 139 (1992); A. Ali and D. London, arXiv:hep-ph/9405283; arXiv:hep-ph/9409399; Z. Phys. C **65**, 431 (1995); S. Herrlich and U. Nierste, Phys. Rev. D **52**, 6505 (1995); M. Ciuchini, E. Franco, G. Martinelli, L. Reina and L. Silvestrini, Z. Phys. C **68**, 239 (1995); A. Ali and D. London, Nuovo Cim. **109A**, 957 (1996); A. Ali, Acta Phys. Polon. B **27**, 3529 (1996); A. J. Buras, arXiv:hep-ph/9711217; A. J. Buras and R. Fleischer, Adv. Ser. Direct. High Energy Phys. **15**, 65 (1998); R. Barbieri, L. J. Hall, S. Raby and A. Romanino, Nucl. Phys. B **493**, 3 (1997); A. Ali and B. Kayser, arXiv:hep-ph/9806230; P. Paganini, F. Parodi, P. Roudeau and A. Stocchi, Phys. Scripta **58**, 556 (1998); F. Parodi, P. Roudeau and A. Stocchi, Nuovo Cim. A **112**, 833 (1999); F. Caravaglios, F. Parodi, P. Roudeau and A. Stocchi, arXiv:hep-ph/0002171; S. Mele, Phys. Rev. D **59**, 113011 (1999); A. Ali and D. London, Eur. Phys. J. C **9**, 687 (1999); M. Ciuchini, E. Franco, L. Giusti, V. Lubicz and G. Martinelli, Nucl. Phys. B **573**, 201 (2000); M. Bargiotti *et al.*, *La Rivista del Nuovo Cimento* **Vol. 23N3** (2000) 1; S. Plaszczynski and M. H. Schune, arXiv:hep-ph/9911280; S. Mele, in *Proc. of the 5th International Symposium on Radiative Corrections (RADCOR 2000)* ed. Howard E. Haber, arXiv:hep-ph/0103040; A. Hocker, H. Lacker, S. Laplace and F. Le Diberder, Eur. Phys. J. C **21** (2001) 225; M. Ciuchini, Nucl. Phys. Proc. Suppl. **109B** (2002) 307; A. Hocker, H. Lacker, S. Laplace and F. Le Diberder, AIP Conf. Proc. **618** (2002) 27; F. Caravaglios, P. Roudeau and A. Stocchi, Nucl. Phys. B **633** (2002) 193; A. J. Buras, arXiv:hep-ph/0210291; G. P. Dubois-Felsmann, D. G. Hitlin, F. C. Porter and G. Eigen, arXiv:hep-ph/0308262; arXiv:hep-ex/0312062; A. Stocchi, arXiv:hep-ph/0405038; J. Charles *et al.* [CKMfitter Group Collaboration], arXiv:hep-ph/0406184.

[4] HFAG: `http://www.slac.stanford.edu/xorg/hfag/`

[5] "THE CKM MATRIX AND THE UNITARITY TRIANGLE". *Based on the First Workshop on "CKM Unitarity Triangle" held at CERN, 13-16 February 2002.* Edited by: M. Battaglia, A. Buras, P. Gambino and A. Stocchi. To be published as **CERN Yellow Book** (hep-ph/0304132).

[6] Proceedings of the Second Workshop on "CKM Unitarity Triangle" *held in Durham, 5-9 April 2003.* Edited by: P. Ball, P. Kluit, J. Flynn and A. Stocchi.

[7] C. Dib, I. Dunietz, F. Gilman, Y. Nir, *Phys. Rev.* **D41** (1990) 1522; G. Buchalla, A.J. Buras and M.E. Lautenbacher, *Rev. Mod. Phys.* **68** (1996) 1125; A. Ali and D. London, in Proceeding of "ECFA Workshop on the Physics of a B Meson Factory", Ed. R. Aleksan, A. Ali (1993); A. Ali and D. London, *Nucl. Phys.* **54A** (1997) 297.

[8] M. Gronau and D. London, *Phys. Lett.* **B253**, 483 (1991); M. Gronau and D. Wyler, *Phys. Lett.* **B265**, 172 (1991); I. Dunietz, *Phys. Lett.* **B270**, 75 (1991); I. Dunietz, *Z. Phys.* **C56**, 129 (1992); D. Atwood, G. Eilam, M. Gronau and A. Soni, *Phys.*

Lett. **B341**, 372 (1995); D. Atwood, I. Dunietz and A. Soni, *Phys. Rev. Lett.* **78**, 3257 (1997).

[9] A. Giri, Yu. Grossman, A. Soffer and J. Zupan, *Phys. Rev.* **D68**, 054018 (2003).

[10] A. Poluektov *et al.* [Belle Collaboration], arXiv:hep-ex/0406067.

[11] M. Gronau and D. London, Phys. Rev. Lett. **65** (1990) 3381.

[12] O. Long, M. Baak, R. N. Cahn and D. Kirkby, Phys. Rev. D **68** (2003) 034010 [arXiv:hep-ex/0303030].

[13] B. Aubert *et al.* [BABAR Collaboration], arXiv:hep-ex/0309017. K. Abe *et al.* [BELLE Collaboration], arXiv:hep-ex/0308048.

[14] B. Aubert *et al.* [BABAR Collaboration], Phys. Rev. Lett. **92** (2004) 251802 [arXiv:hep-ex/0310037].

[15] Y. Grossman and M. P. Worah, Phys. Lett. B **395** (1997) 241 [arXiv:hep-ph/9612269]; M. Ciuchini, E. Franco, G. Martinelli, A. Masiero and L. Silvestrini, Phys. Rev. Lett. **79** (1997) 978 [arXiv:hep-ph/9704274]; Y. Grossman, G. Isidori and M. P. Worah, Phys. Rev. D **58** (1998) 057504 [arXiv:hep-ph/9708305].

[16] B. Aubert *et al.* [BABAR Collaboration], arXiv:hep-ex/0403026. K. Abe *et al.* [Belle Collaboration], Phys. Rev. Lett. **91** (2003) 261602 [arXiv:hep-ex/0308035]. B. Aubert *et al.* [BABAR Collaboration], arXiv:hep-ex/0403001.

[17] M. Ciuchini, E. Franco, G. Martinelli, M. Pierini and L. Silvestrini, Phys. Lett. B **515** (2001) 33 [arXiv:hep-ph/0104126].

[18] M. Ciuchini, E. Franco, G. Martinelli, A. Masiero, M. Pierini and L. Silvestrini, arXiv:hep-ph/0407073.

[19] M. Ciuchini, E. Franco, F. Parodi, V. Lubicz, L. Silvestrini and A. Stocchi, eConf **C0304052** (2003) WG306 [arXiv:hep-ph/0307195].